Biochimica et Biophysica Acta 1847 (2015) 729–738

Contents lists available at ScienceDirect

Biochimica et Biophysica Acta

journal homepage: www.elsevier.com/locate/bbabio

Acetylation of human mitochondrial citrate carrier modulates mitochondrial citrate/malate exchange activity to sustain NADPH production during macrophage activation

Erika M. Palmieri [a], Iolanda Spera [a], Alessio Menga [a], Vittoria Infantino [d], Vito Porcelli [a], Vito Iacobazzi [a,b,c], Ciro L. Pierri [a], Douglas C. Hooper [e,f], Ferdinando Palmieri [a,b,*], Alessandra Castegna [a,b,**]

[a] Department of Biosciences, Biotechnologies and Biopharmaceutics, University of Bari "Aldo Moro", Bari, Italy
[b] Center of Excellence in Comparative Genomics, University of Bari "Aldo Moro", Bari, Italy
[c] CNR Institute of Biomembranes and Bioenergetics, Bari, Italy
[d] Department of Science, University of Basilicata, Potenza, Italy
[e] Department of Cancer Biology, Thomas Jefferson University, Philadelphia, USA
[f] Department of Neurological Surgery, Thomas Jefferson University, Philadelphia, USA

ARTICLE INFO

Article history:
Received 26 November 2014
Received in revised form 27 March 2015
Accepted 18 April 2015
Available online 24 April 2015

Keywords:
Citrate
Mitochondrial citrate carrier
Acetylation
Post-translational modification
Inflammation
Macrophage

ABSTRACT

The mitochondrial citrate–malate exchanger (CIC), a known target of acetylation, is up-regulated in activated immune cells and plays a key role in the production of inflammatory mediators. However, the role of acetylation in CIC activity is elusive. We show that CIC is acetylated in activated primary human macrophages and U937 cells and the level of acetylation is higher in glucose-deprived compared to normal glucose medium. Acetylation enhances CIC transport activity, leading to a higher citrate efflux from mitochondria in exchange with malate. Cytosolic citrate levels do not increase upon activation of cells grown in deprived compared to normal glucose media, indicating that citrate, transported from mitochondria at higher rates from acetylated CIC, is consumed at higher rates. Malate levels in the cytosol are lower in activated cells grown in glucose-deprived compared to normal glucose medium, indicating that this TCA intermediate is rapidly recycled back into the cytosol where it is used by the malic enzyme. Additionally, in activated cells CIC inhibition increases the $NADP^+$/NADPH ratio in glucose-deprived cells; this ratio is unchanged in glucose-rich grown cells due to the activity of the pentose phosphate pathway. Consistently, the NADPH-producing isocitrate dehydrogenase level is higher in activated glucose-deprived as compared to glucose rich cells. These results demonstrate that, in the absence of glucose, activated macrophages increase CIC acetylation to enhance citrate efflux from mitochondria not only to produce inflammatory mediators but also to meet the NADPH demand through the actions of isocitrate dehydrogenase and malic enzyme.

1. Introduction

Among the mechanisms regulating cell metabolism, reversible acetylation of the ε-amino group of internal lysine (acetylation) has emerged as a mechanism playing a crucial role in regulating the function of non-histone proteins such as transcription factors and metabolic enzymes [1]. In particular acetylation/deacetylation of mitochondrial proteins most likely represents one mechanism by which mitochondrial functions are tailored to meet the demand of metabolic challenges [2]. Novel findings from acetylome studies [1] have identified as targets of acetylation proteins belonging to the mitochondrial carrier family (MCF), which transport important metabolites into and out of mitochondria [3,4]. One of these targets is the mitochondrial citrate carrier (CIC), which catalyses the export of citrate from the mitochondrial matrix in exchange for cytosolic malate [5–7]. This transporter is essential for fatty acid biosynthesis because citrate in the cytosol is cleaved to acetyl-CoA and oxaloacetate by citrate lyase. Acetyl-CoA is directly used for fatty acid synthesis, and oxaloacetate produces NADPH plus H^+ (also necessary for fatty acid production) via malate dehydrogenase and malic enzyme [8]. However, the role of acetylation on this protein function is not known. Recently it has been shown that CIC expression

Abbreviations: CIC, citrate carrier; MCF, mitochondrial carrier family; PPP, pentose phosphate pathway; IDH1, isocitrate dehydrogenase; CNSB, 4-chloro-3-[(3-nitrophenyl)amino]sulfonyl benzoic acid; PMS, post-mitochondrial supernatant; NAM, nicotinamide; AcCIC, acetylated CIC

* Correspondence to: F. Palmieri, Department of Biosciences, Biotechnologies and Biopharmaceutics, University of Bari "Aldo Moro", Via Orabona 4, Bari 70125, Italy.
** Correspondence to: A. Castegna, Department of Biosciences, Biotechnologies and Biopharmaceutics, University of Bari "Aldo Moro", Via Orabona 4, Bari 70125, Italy. Tel.: +39 080 5442771; fax: +39 080 5442770.
E-mail addresses: alessandra.castegna@uniba.it (A. Castegna), ferdinando.palmieri@uniba.it (F. Palmieri).

http://dx.doi.org/10.1016/j.bbabio.2015.04.009
0005-2728/

increases in activated immune cells and plays a key role in the production of inflammatory mediators [9,10]. This seminal finding is crucial to understand macrophage metabolism, although further information on how this carrier activity is modulated during the complex metabolic activation of macrophages is lacking. In the present study we show that CIC is acetylated in activated human macrophages and histiocytoma U937 cells and the level of acetylation is dependent on the available carbon sources, increasing when glucose is absent. We provide evidence that CIC acetylation increases citrate efflux in exchange with malate, to respond to the increasing cellular NAPDH demand. Lack of glucose diverts NADPH production from the pentose phosphate pathway (PPP) to the malic enzyme [11] and $NADP^+$-isocitrate dehydrogenase (IDH1), making NADPH availability strictly dependent on citrate efflux. Activated cells respond to this request by increasing the acetylation of CIC, which results in a net increase of cytosolic citrate. This mechanism is essential in a low glucose environment, in which immune cells need to reprogram metabolism to sustain the many cellular functions typical of their activation.

2. Materials and methods

2.1. Cell growth

Human blood samples were obtained from healthy individuals at Thomas Jefferson University Hospital under an Institutional Review Board approved protocol. Human monocytes were isolated by using CD14 MicroBeads (Miltenyi Biotec) [12]. Monocytes were seeded in RPMI 1640 medium supplemented with 10% (*v*/*v*) fetal bovine serum, 2 mM l-glutamine, 100 units of penicillin and 100 μg/mL streptomycin at 37 °C in 5% CO_2 at a concentration of 6×10^5 cells/mL. Differentiation was carried out as previously described [9]. Histiocytoma U937 cells (ICLC HTL 94002-Interlab Cell Line Collection) were cultured as described above. Right before activation both primary macrophages and U937 cells were transferred into a either glucose or glucose-free medium and activated with 2 μg/mL bacterial LPS (Sigma) or with 5 ng/mL of TNFα and 10 ng/mL of IFNγ (Immunotools) for 24 h [9,10]. As acetylation control, human macrophages incubated in glucose or glucose-less medium were treated with the deacetylase inhibitor 10 mM nicotinamide alone (NAM, Sigma) for 24 h [13]. CIC was inhibited in U937 cells by adding 1 μM of the specific CIC inhibitor 4-chloro-3-[(3-nitrophenyl)amino]sulfonyl benzoic acid (CNSB, Millipore) [6] 1 h before activation.

2.2. Immunoprecipitation and Western blotting of CIC carrier

For CIC immunoprecipitation cell pellets (5×10^6 cells) were resuspended in 1 mL of denaturing lysis buffer (1% SDS, 5 mM EDTA, 50 mM Tris–HCl, pH 7.4) and the lysates centrifuged for 15 min at 20,000 ×*g*. After the supernatants were diluted with 50 mM Tris–HCl, 100 mM NaCl and 1% Triton X-100, rabbit antiserum directed against CIC carrier was added, and the mixture was incubated with shaking for 1 h at 4 °C. Then 75 μL Protein G microbeads (Miltenyi Biotech) were added; after mixing, samples were incubated with shaking for 30 min at 4 °C. For magnetic immunoseparation beads were incubated with 20 μL of 1× SDS-PAGE sample buffer (1% SDS, 50 mM Tris–HCl pH 6.8, 50 mM DTT, 10% glycerol, 0.005% bromophenol blue). Elution of the immunoprecipitated protein was carried out by adding a further 30 μL of elution buffer.

For SDS-PAGE of immunoprecipitates, eluted proteins were incubated at 95 °C for 5 min. Then the same amount of eluted proteins from each sample was loaded in two different lanes of a continuous 12% SDS PAGE. The electrophoresed proteins were blotted on a nitrocellulose membrane and probed with anti-acetyl-lysine antibody (Santa Cruz Biotechnology) or CIC antibody. The immunoprecipitated proteins were visualized through the immunoreaction of the goat anti-rabbit secondary antibody detected by the Immobilon Western chemiluminescent kit (Millipore) and normalized against β-actin protein levels.

2.3. Construction of expression vector harboring SIRT3 complete coding sequence (CDS) and transient transfection in U937 cells

1 μg of human liver total RNA (AM7960, Life Technologies) was reverse transcribed with GeneAmp RNA PCR core kit (Applied Biosystem) as described previously [14]. The full-length coding region of the human SIRT3 (GenBank accession number NM_012239.5) was amplified from Liver cDNA using the iProof High Fidelity DNA Polymerase (Bio-Rad), GC Buffer, dimethyl sulfoxide (DMSO), dNTPs, a 5′-primer (5′ CAGGAA TTCATGGCGTTCTGGGGTTGGCGCG 3′) and a 3′-primer (5′ CGACTCGA GCTATTTGTCTGGTCCATCAAGCTT 3′) in a final volume of 50 μL (Infantino et al., 2013). The fragment was then cloned into pcDNA3.1(+) vector (Invitrogen) in the sense orientation. The fidelity of the final human SIRT3 insert in pcDNA3.1(+) plasmid was verified by DNA sequencing using BigDye Terminator Kit (Applied Biosystems).

U937 cells were transfected with the pcDNA3.1(+) vector containing the target SIRT3 DNA sequence by FuGENE HD Transfection Reagent (PROMEGA) according to the manufacturer's instructions. In brief, U937 cells were plated the day of transfection at a density of 1×10^7 cells into a T-150 flask and grown in 47 mL of RPMI medium with 10% FBS and 1% penicillin/streptomycin. The mixture of plasmid (24 μg) and transfection reagent (144 μL) in Opti-MEM medium without serum (Recommended Reagent:DNA ratio for U937 cells is 6:1) was added to the culture and the cells were incubated for 48 h. Two days later, transfected cells were used in the experiments. The transfection efficiency was analyzed by immunoblotting with anti-sirt3 antibody (SantaCruz Biotechnology). Where indicated transfected cells, were also treated with nicotinamide (NAM, Sigma) for 24 h at the concentration of 10 mM.

2.4. Reconstitution of solubilized mitochondria and transport measurements

Mitochondria (0.41 mg/mL), isolated as described [15] were solubilized in 3% Triton X-114, 50 mM NaCl, 1 mM EDTA, 10 mM HEPES pH 7.2. After 20 min at 0 °C, the mixture was spun at 100,000 ×*g* for 10 min. The supernatant (extract) was reconstituted into phospholipid vesicles (liposomes) by cyclic removal of the detergent using a hydrophobic column [16]. The composition of the initial mixture used for reconstitution was: 70 μL of mitochondrial extract, 57 μL of 10% Triton X-114, 100 μL of 10% phospholipids in the form of sonicated liposomes [17], 10 mM citrate, 0.6 mg cardiolipin, 20 mM HEPES, pH 7.2, and water to a final volume of 700 μL. These components were mixed thoroughly, and the mixture was recycled 13 times through an Amberlite column (3.2 × 0.5 cm) pre-equilibrated with the same buffer and the same concentration of the substrate (except where otherwise indicated) present in the reconstitution mixture. External substrate was removed from proteoliposomes on a Sephadex G-75 column preequilibrated with a buffer containing 50 mM NaCl and 10 mM Hepes, pH 7.2. Transport at 25 °C was started by adding 1 mM [^{14}C]citrate to the proteoliposomes and terminated by the addition of 20 mM pyridoxal 5′-phosphate, an inhibitor of several mitochondrial carriers [18–20]. In controls, carrier-mediated transport was inhibited by addition of pyridoxal phosphate together with the labeled substrate [21]. The external radioactivity was removed on Sephadex G-75 and the internal radioactivity was measured. The transport activity was the difference between experimental and control values.

Transport assays with isolated mitochondria were performed as described [22] with some modifications. Briefly, mitochondria (0.6 mg) were incubated in a buffer containing 100 mM KCl, 20 mM HEPES, pH 7.0, and 2 μg of rotenone. Transport at 9 °C was performed adding 1 mM of [^{14}C]citrate to mitochondria and terminated after 15 s by adding 20 mM BTA (benzene-1,2,3-tricarboxylate). Mitochondria were pelleted, suspended with water and extracted with $HClO_4$; and the extracts were used for scintillation counting of ^{14}C.

2.5. Molecular modeling of citrate carrier K97 acetylation

Modeller was used to calculate three dimensional structural models of human CIC coded by the SLC25A1 gene using the structure of the bovine BtAAC1 (protein data bank accession code: 1okc) as template for the comparative modeling as previously described for CIC and other mitochondrial carriers [4,23]. For citrate docking analysis, citrate ligand was docked into the predicted binding sites using Autodock 1.5.2 as previously described [23]. Experimentally detected post-translational modifications of citrate carrier were recovered from the PhosphoSitePlus resource (http://www.phosphosite.org). The acetylation of K97 was introduced in the 3D protein model with the Molefacture tool (http://www.ks.uiuc.edu/Research/vmd/) as previously described for other carriers [4].

2.6. Liquid chromatography tandem mass spectrometry analysis (LC-MS/MS) of metabolites in U937 cells

For mass spectrometry analysis fast separation of post-mitochondrial supernatant (PMS) was achieved as described [15]. Volumes corresponding to 2 mg of proteins from PMS were extracted as indicated [15,24–27]. A Quattro Premier mass spectrometer interfaced with an Acquity UPLC system (Waters) was used for LC-MS/MS analysis as described [24,26–29]. Calibration curves were established using standards, processed under the same conditions as the samples, at five concentrations. The best fit was determined using regression analysis of the peak analyte area. The multiple reaction monitoring transitions in the positive ion mode were m/z 744.06 > 507.83 for $NADP^+$ and m/z 746.02 > 729.00 for NADPH. The MRM transitions monitored in the negative ion mode for TCA intermediates were m/z 190.95 > 110.89 for citrate and m/z 132.95 > 115.20 for malate. The flow rate was 0.3 mL/min.

2.7. Real-time PCR

Total RNA was extracted from 1×10^6 U937 cells activated in the presence or absence of glucose and reverse transcribed as described [30]. Real-time PCR was performed as described [31,32]. Taq-man probes for human IDH1, and human β-actin were purchased from Applied Biosystems. All transcript levels were normalized against the β-actin expression level.

3. Results

3.1. CIC acetylation in differentiated and LPS- or TNFα/IFNγ-treated human macrophages

Since CIC is known to be acetylated in humans [1] we investigated whether CIC is a target of acetylation in primary human monocyte-derived macrophages. We first immunoprecipitated the CIC carrier from macrophages as described in the Methods section. Immunoprecipitated samples displayed a major band at 33 kDa corresponding to the carrier molecular weight (Fig. 1). The level of CIC acetylation was tested in activated macrophages in the presence (Fig. 2a) or absence of glucose (Fig. 2b). Both sets of samples were processed for CIC immunoprecipitation and Western blotting exactly in the same way, and the levels of acetylated CIC normalized to total CIC (AcCIC/CIC ratio) were evaluated. In glucose-rich medium LPS or TNFα/IFNγ activation induced a small decrease in AcCIC/CIC ratio, due to the increase of CIC expression without a significant change in the acetylation levels. Switching control cells from glucose-rich to glucose-less medium produced a slight increase in AcCIC/CIC ratio (Fig. 2b and c). LPS or TNFα/IFNγ-activated cells grown without glucose displayed a 52 and 70% increase, respectively, in AcCIC/CIC ratio compared to the corresponding activated cells in glucose-rich medium (Fig. 2c). As a positive control, cells were treated with the deacetylase inhibitor NAM (in the absence of LPS or TNFα/

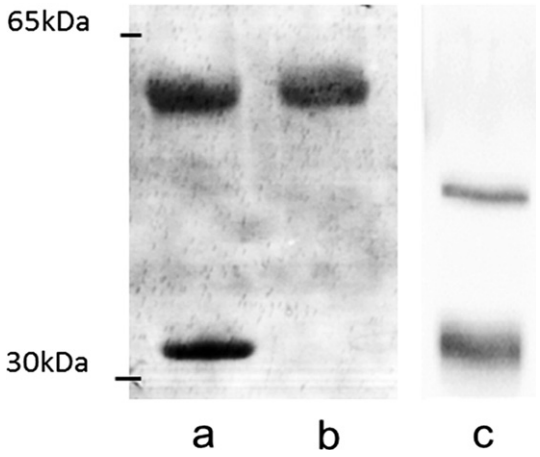

Fig. 1. Immunoprecipitation of CIC from human macrophages. (a) SDS-PAGE of the immunoprecipitated protein sample shows the target protein at 33 kDa (the CIC protein) and a 55 kDa band, which is the denatured heavy antibody chain. (b) SDS-PAGE of the CIC antibody shows the band at 55 kDa. (c) Western blotting and immunostaining of mitochondrial extracts with the CIC antibody indicate a major band at 33 kDa.

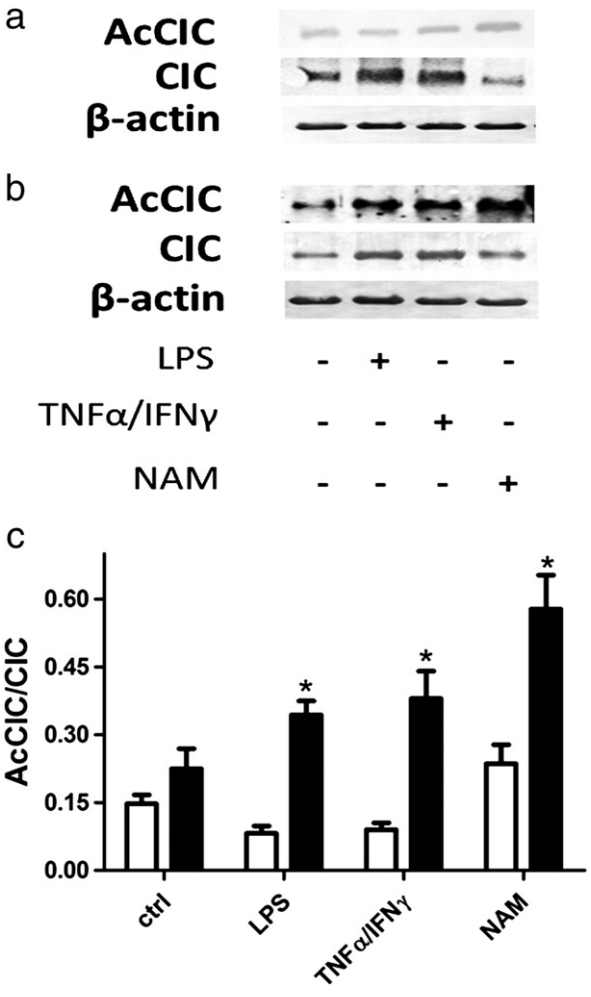

Fig. 2. Acetylation levels of CIC in activated human macrophages in high glucose or glucose-free medium. CIC was immunoprecipitated from primary human monocytes-derived macrophages, treated for 24 h with LPS, TNFα/IFNγ or NAM in (a) glucose-rich or (b) glucose-free conditions, and probed with anti-CIC and anti-acetyl-lysine antibody. (c) CIC acetylation levels in glucose-rich (white bars) or glucose-free (black bars) medium are normalized to total CIC protein amount and are reported as AcCIC/CIC means ± S.E.M. of six independent experiments. Significant differences of the CIC acetylation levels in cells treated in glucose-free compared to glucose rich medium (*$p < 0.05$, one-way ANOVA) and NAM compared to LPS or TNFα/IFNγ are indicated ($^{\#}p < 0.05$, one-way ANOVA).

IFNγ), which produced a strong increase in the basal acetylation of CIC in both glucose grown- or glucose deprived-cells (Fig. 2c).

3.2. CIC acetylation in TNFα/IFNγ-activated U937 cells

To obtain insight into the role of the acetylation with respect to the citrate/malate exchange features of CIC we used the U937 histiocytic lymphoma cells, a model cell line that matures in response to a number of soluble stimuli, adopting the morphology and characteristics of monocytes/macrophages. We used the combination of TNFα and IFNγ as activatory stimulus since it produced a similar or more prominent effect than LPS on CIC acetylation in activated macrophages (Fig. 2). The level of CIC acetylation was tested in activated U937 cells in the presence (Fig. 3a) or absence of glucose (Fig. 3b). Switching control cells from glucose-rich to glucose-free medium did not produce any significant change in Ac-CIC/CIC ratio (Fig. 3c). TNFα/IFNγ-activated cells grown in the absence of glucose displayed a 50% increase in Ac-CIC/CIC ratio compared to similarly activated cells grown in glucose-rich medium (Fig. 3c).

3.3. CIC transport activity in TNFα/IFNγ-activated U937 cells grown in conditions of glucose rich and deprived medium

We tested the activity of CIC in mitochondrial extracts from U937 cells grown in normal or glucose-free medium as performed for other mitochondrial carriers [15,33,34]. As shown in Fig. 4 the uptake of radioactive citrate (normalized to the amount of CIC protein) in liposomes reconstituted with mitochondrial extract from TNFα/IFNγ-treated cells grown in the absence of glucose (measured as [^{14}C]citrate/citrate homoexchange, the distinctive transport of CIC) was markedly

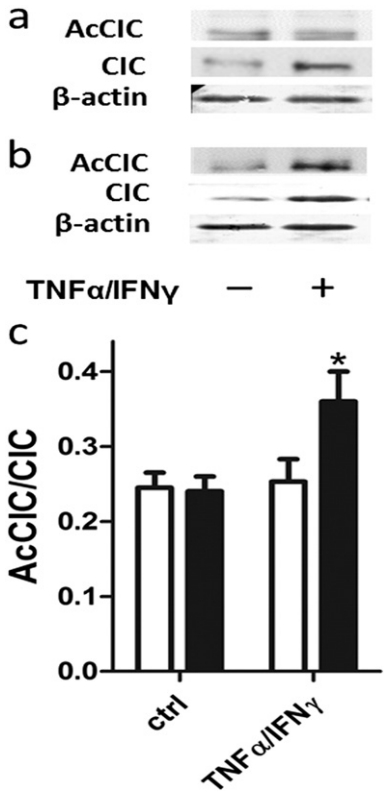

Fig. 3. Acetylation levels of CIC in activated U937 cells in high glucose or glucose-free medium. CIC was immunoprecipitated from U937 cells, treated for 24 h with TNFα/IFNγ in (a) glucose-rich or (b) glucose-deprived conditions, and probed with anti-CIC and anti-acetyl-lysine antibody. (c) Acetylation levels of CIC normalized to total CIC are reported as means ± S.E.M. of at least three independent experiments. Significant differences of the CIC acetylation levels in cells treated in glucose-deprived compared to glucose rich cells are indicated (*p < 0.05, one-way ANOVA).

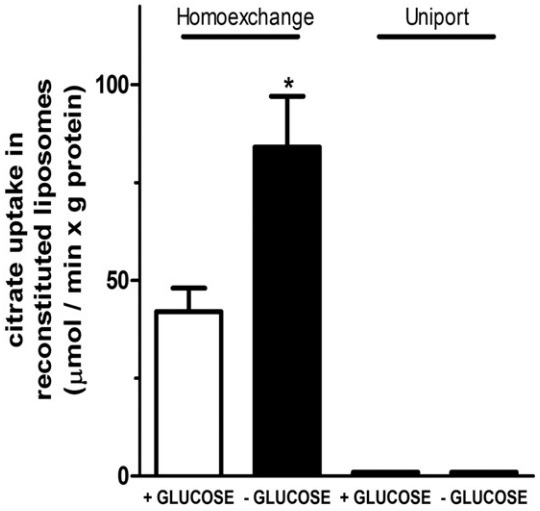

Fig. 4. Functional characterization of CIC from mitochondria of U937 cells grown in the presence or absence of glucose. The uptake rate of [^{14}C] citrate was measured by adding 1 mM of [^{14}C] citrate to proteoliposomes reconstituted with mitochondrial extracts from U937 cells activated with TNFα/IFNγ in normal or glucose-deprived medium in the presence or absence of internal citrate (uniport). The means and S.E.M. from four independent experiments are shown (*p < 0.01, one-way ANOVA).

increased as compared with those reconstituted with the mitochondrial extract from TNFα/IFNγ-treated cells grown in normal medium (84.0 ± 13.0 versus 42.0 ± 6.0 μmol of citrate/min x g of protein, respectively, $p < 0.001$). Uptake of [^{14}C]citrate without internal citrate was negligible in both conditions.

To evaluate whether the acetylation of CIC influences the K_m and/or the V_{max}, the kinetic constants of CIC in liposomes reconstituted with mitochondrial extracts from TNFα/IFNγ-activated cells grown in the presence or absence of glucose were determined by measuring the activity at varius [^{14}C]citrate concentrations in the presence of a fixed saturating concentration of internal citrate.

The V_{max} value of CIC in liposomes reconstituted with mitochondrial extracts from cells activated in glucose-free medium was substantially higher than that determined in liposomes reconstituted with mitochondrial extracts from activated cells in normal medium (89.5 ± 19.6 μmol/min ×g of protein versus 37.0 ± 5.4 μmol/min ×g of protein). By contrast, the K_m values of CIC for citrate were similar in both growth conditions (60.0 ± 5.1 versus 63.0 ± 7.1 μM, $p < 0.01$). Therefore CIC acetylation increases the maximal activity of the transport without changing its K_m for citrate.

3.4. CIC acetylation in resting and SIRT3-overexpressing U937 cells

To provide more evidence in favor of the role of CIC acetylation on its transport activity, the effect of NAM on CIC acetylation and transport was tested in both control and pcDNA3-SIRT3 overexpressing U937 cells grown in glucose rich medium but in the absence of LPS or TNFα/IFNγ. The AcCIC/CIC ratios significantly increased in NAM treated compared to untreated U937 cells (Fig. 5a). Furthermore, NAM treated pcDNA3-SIRT3 cells displayed significantly higher AcCIC/CIC ratios compared to SIRT3-overexpressing cells (Fig. 5b). CIC protein levels were unchanged in both cases (Fig. 5a-b).

The effect of NAM on CIC transport activity in mitochondrial extracts from control and pcDNA3-SIRT3 overexpressing U937 cells was then evaluated. With NAM control cell-derived mitochondria exhibited a significant increase in CIC transport activity compared to untreated cells (17.33 ± 0.50 versus 12.90 ± 1.50 μmol of citrate/min ×g of protein, respectively, $p < 0.01$) (Fig. 5c). These results parallel the acetylation levels of CIC measured under the same conditions (Fig. 5a). A greater increase in CIC activity was observed using mitochondrial extracts from NAM-treated compared to untreated SIRT3 overexpressing U937 cells

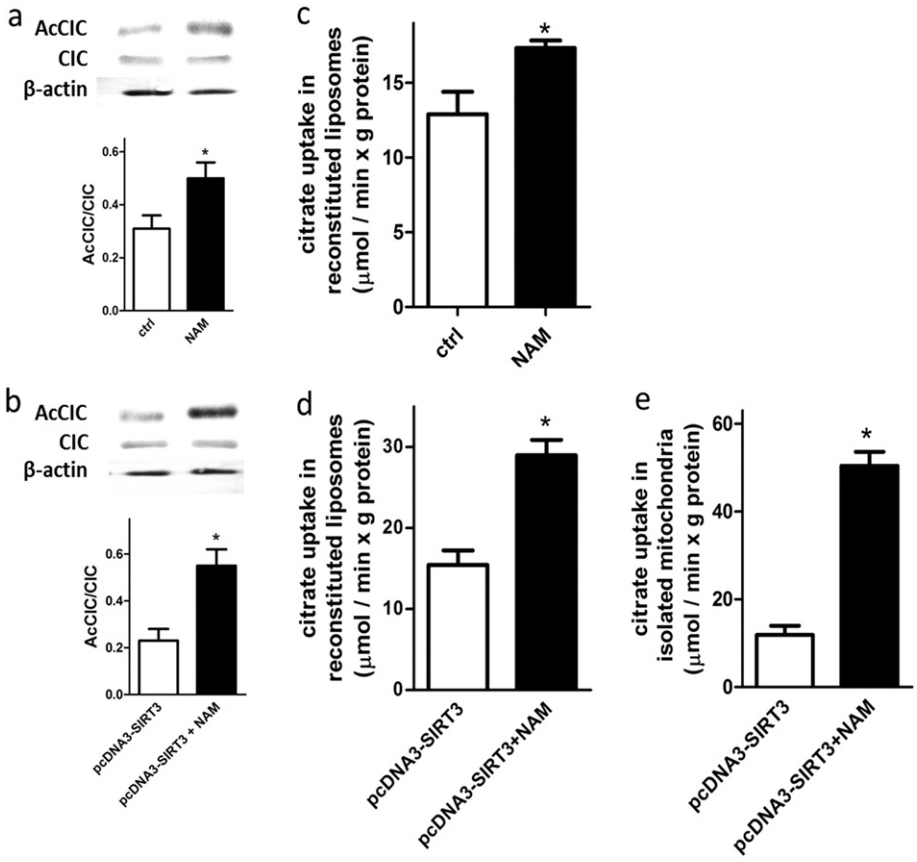

Fig. 5. Functional characterization of acetylated CIC. CIC was immunoprecipitated from control (a) and pcDNA3-SIRT3 transfected U937 cells (b) in the absence or presence of 10 mM NAM and probed with anti-CIC and anti-acetyl-lysine antibody. Normalized acetylation levels of CIC are reported as means ± S.E.M. of three independent experiments. Significant differences of the CIC acetylation levels in NAM-treated compared to control cells and NAM-treated compared to NAM-untreated SIRT3 overexpressing cells are indicated (*$p < 0.05$, one-way ANOVA). (c–d) The uptake rate of [^{14}C] citrate was measured by adding 1 mM of [^{14}C] citrate to proteoliposomes reconstituted with mitochondrial extracts from control and NAM treated (c), pcDNA3-SIRT3 transfected and pcDNA3-SIRT3/NAM-treated resting U937 cells (d) in the presence or absence of internal citrate (uniport). (e) The uptake rate of [^{14}C] citrate was measured by adding 1 mM of [^{14}C] citrate to intact mitochondria isolated from pcDNA3-SIRT3 and NAM-treated pcDNA3-SIRT3 U937 cells. The means and S.E.M. from three independent experiments are shown (*$p < 0.01$, one-way ANOVA).

(29.25 ± 1.90 versus 15.45 ± 1.79 μmol of citrate/min ×g of protein, respectively, $p < 0.01$) (Fig. 5d). All these results parallel the acetylation levels of CIC measured under the same conditions (Fig. 5b).

To exclude the possibility that acetylation affects the reconstitution of CIC into liposomes, we measured the transport of radioactive citrate into intact mitochondria isolated from pcDNA3-SIRT3 transfected cells treated or untreated with NAM. Also in these experiments the uptake of [^{14}C]citrate was markedly increased in NAM-treated compared to NAM-untreated SIRT3 overexpressing cells (50.4 ± 3.2 versus 11.3 ± 2.1 μmol of citrate/min ×g of protein, $p < 0.01$) (Fig. 5e), indicating that the increase of CIC transport activity reflecting the levels of the carrier acetylation is not an artifact linked to the reconstitution procedure used in the present work.

3.5. Molecular modeling of CIC acetylated in K97

We investigated the influence of the acetylation of K97, found to be acetylated in human CIC [1], on citrate binding in order to provide a molecular explanation of the increased V_{max} in acetylated cells. K97 is located close to residues of the proposed citrate binding site [4,23] and appears to participate in citrate binding (Fig. 6a-b) together with residues R282 and R285. The putative acetylation of K97 would allow a better fitting of the proposed binding region due to the strengthening of citrate interactions with basic residues R282 and R285. Furthermore, the acetylation of K97 produces a different network of interactions among citrate, residues of the proposed binding region and residues of the matrix gate (m-gate) (Fig. 6a-b).

3.6. Citrate and malate levels in the PMS of TNFα/IFNγ-activated U937 cells in conditions of glucose-rich versus glucose-deprived medium

To ascertain whether CIC acetylation modifies citrate and malate levels in the cytosol we measured these metabolites in the PMS of TNFα/IFNγ-activated compared to resting U937 cells grown in the presence or absence of glucose.

In glucose-rich medium, cytosolic levels of citrate were significantly higher in activated compared to resting U937 cells (Fig. 7a), consistent with the increased CIC gene expression during immune activation [9,10]. As expected, upon CIC inhibition citrate levels were reduced almost to the control ones (Fig. 7a). Cytosolic levels of malate were significantly higher in activated- compared to resting-U937 cells (Fig. 7c), suggesting that, in the presence of glucose, PPP is activated and malate is not rapidly consumed by the malic enzyme. A further significant increase in cytosolic malate was measured in the presence of CNSB (Fig. 7c), suggesting that following CIC inhibition, malate cannot enter mitochondria in exchange with citrate, but is probably transported back from mitochondria in place of citrate by the dicarboxylate carrier (DIC).

In glucose-free medium control levels of citrate (Fig. 7b) are lower compared to the levels of this metabolite measured in glucose-rich medium (Fig. 7a). Citrate did not accumulate in the cytosol of activated-compared to resting-U937 cells (Fig. 7b) and upon CIC inhibition citrate levels were more strongly reduced in glucose-free versus glucose-rich media (Fig. 7b). This indicates that in cells activated in the absence of glucose citrate is probably being consumed at very high rates. Malate

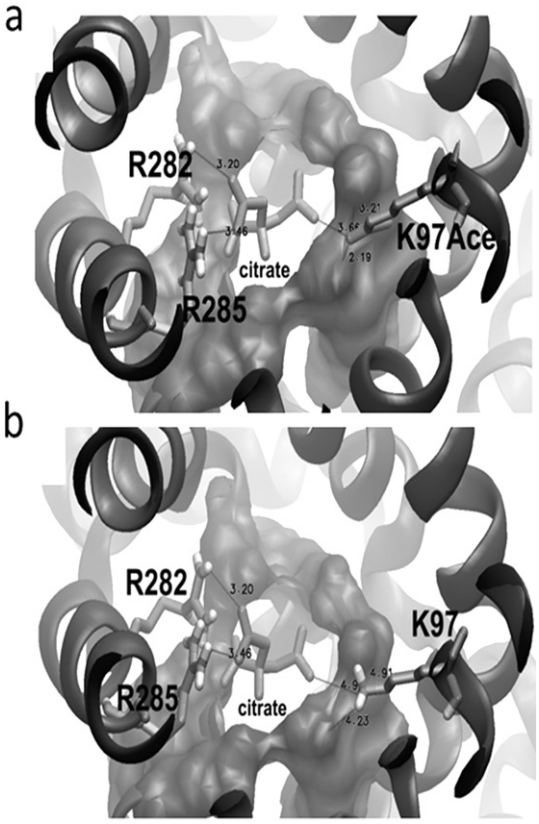

Fig. 6. Molecular modeling of acetylated CIC at K97. The exploded view of citrate carrier cavity is reported in grey cartoon representation. Residues of the proposed binding region (K97, R282, R285) and citrate ligand are reported in sticks representation and indicated by black labels. Residues forming the matrix gate are reported in gray surf representation. In panel a is possible to see K97 acetylated. Ionic and H-bond interactions between residues of the proposed binding region, the citrate ligand and residues of the matrix gate are represented with dashed lines and black labels.

levels were significantly lower in the cytosol of activated-compared to resting-U937 cells (Fig. 7d). Activation in the presence of the CIC inhibitor reinstated malate levels only to those of the control samples (Fig. 7d), indicating that malate, under these conditions, is more rapidly metabolized by the malic enzyme, which is essential for NADPH production in the absence of glucose [35,36].

3.7. $NADP^+$/NADPH ratios in the PMS of TNFα/IFNγ-activated U937 cells in conditions of glucose-rich versus glucose-deprived medium

Since NADPH is an important factor in immune cell activation regardless of the cell growth conditions, its levels may be dependent on CIC activity when glucose is not available. To determine if this was the case we quantified the levels of NADPH and $NADP^+$ in TNFα/IFNγ-activated compared to resting U937 cells grown in the presence or absence of the CIC inhibitor CNSB in conditions supporting different levels of CIC acetylation. Upon TNFα/IFNγ activation in the presence of glucose $NADP^+$/NADPH ratios were decreased compared to resting cells (Fig. 8a). A similar decrease was displayed by activated cells treated with the CIC inhibitor (Fig. 8a). In the absence of glucose availability, the $NADP^+$/NADPH control ratio (Fig. 8b) was higher compared to that measured in high glucose (see Fig. 8a). Furthermore, the $NADP^+$/NADPH ratio was significantly elevated by activating the cells and even higher when the activated cells were treated with the CIC inhibitor (Fig. 8b), indicating that the contribution of citrate transport from mitochondria is important for NADPH synthesis. In all cases the total amount of the phosphorylated pyrimidine coenzymes ($NADP^+$ + NADPH) was similar (Fig. 8c–d).

3.8. Isocitrate dehydrogenase expression levels in TNFα/IFNγ-activated U937 cells in conditions of glucose-rich versus glucose-deprived medium

To ascertain whether alternative pathways to produce NADPH are induced in activated U937 cells grown in free versus rich glucose medium, we assessed mRNA levels of IDH1, a $NADP^+$-dependent citrate to oxoglutarate converting enzyme that is known to be suppressed in cells undergoing a pro inflammatory stimuli [37]. Compared to IDH1 mRNA levels in control, unstimulated cells, a decrease of about 4-fold was observed in U937 cells activated in glucose-rich medium (Fig. 9a). Surprisingly, an increase of approximately 1.6-fold of IDH1 mRNA was observed in U937 cells activated in glucose-free medium as compared to similarly cultured control cells (Fig. 9b).

4. Discussion

Among the carrier proteins present in the inner membrane of mitochondria, the citrate transport system (CIC) plays an important role in fatty acid synthesis, gluconeogenesis, and the transfer of reducing equivalents across the inner mitochondrial membrane. According to previously published data on the protein isolated from rat liver and reconstituted into liposomes [6,7,38] CIC catalyzes the efflux of citrate, together with a proton, from the matrix to the cytosol in an electroneutral exchange for another tricarboxylate-H^+, malate, or phosphoenolpyruvate [39]. The proposed mechanism of transport is sequential [39], which implies the obligatory presence of a counter substrate for citrate efflux. The citrate/malate antiport fulfills important metabolic demands [40]. Citrate is a key substrate for the generation of energy and a modulator of several enzymatic activities. In the mitochondria citrate is oxidized *via* the Krebs cycle and Oxidative Phosphorylation (OXPHOS). In the cytoplasm citrate inhibits glycolysis while supporting lipid synthesis and the reduction of $NADP^+$ [41,42]. Recent data have shown that CIC expression is increased in INS-1 cells challenged with insulin [43], in cancer [44,45] and in activated macrophages during inflammation [9].

Extensive reports support the concept that immune cells are adapted to use different nutrient sources [46]. It is known that glucose contributes to 60% of an immune cell's energy needs, the remaining 40% being satisfied by glutamine [11]. Macrophages consume very high amounts of glucose although only 10% is oxidized [35], whereas glutamine is oxidized at high rates [11,35]. Both energy substrates can produce high amounts of NADPH through different NADPH-generating pathways. When glutamine is used to produce new amino acids in periods of active synthesis and secretion, glucose is diverted to the PPP for NADPH synthesis [11]. Conversely, a considerable proportion of NADPH is produced *via* glutamine metabolism when glucose 6-phosphate dehydrogenase is inhibited in macrophages by adrenaline [35], or during periods of active pinocytosis and phagocytosis, in which glucose carbon may be diverted toward lipid synthesis [11]. The inflammatory response is nutritionally challenged in conditions of low glucose availability, as the cellular NADPH demand cannot be sustained by the PPP. Alternative sources of NADPH require high cytosolic levels of citrate. Indeed this TCA intermediate can be converted to malate, which is substrate of the NADPH-producing malic enzyme, or can be direct substrate of the $NADP^+$-dependent isocitrate dehydrogenase, although its expression has been shown to be suppressed under pro inflammatory challenge [37]. In both cases NADPH production becomes more dependent on citrate efflux from mitochondria.

Our data demonstrate that in conditions of glucose deprivation cells respond to activation with proinflammatory cytokines by promoting a novel mechanism of post-translational control of CIC activity that influences the rate of citrate efflux. CIC is more acetylated in activated macrophages grown in the absence of glucose compared to those grown in normal glucose. Acetylation increases the rate of citrate efflux from mitochondria in exchange for cytosolic malate thereby assuring NADPH production. Indeed in activated cells treated with the CIC inhibitor the

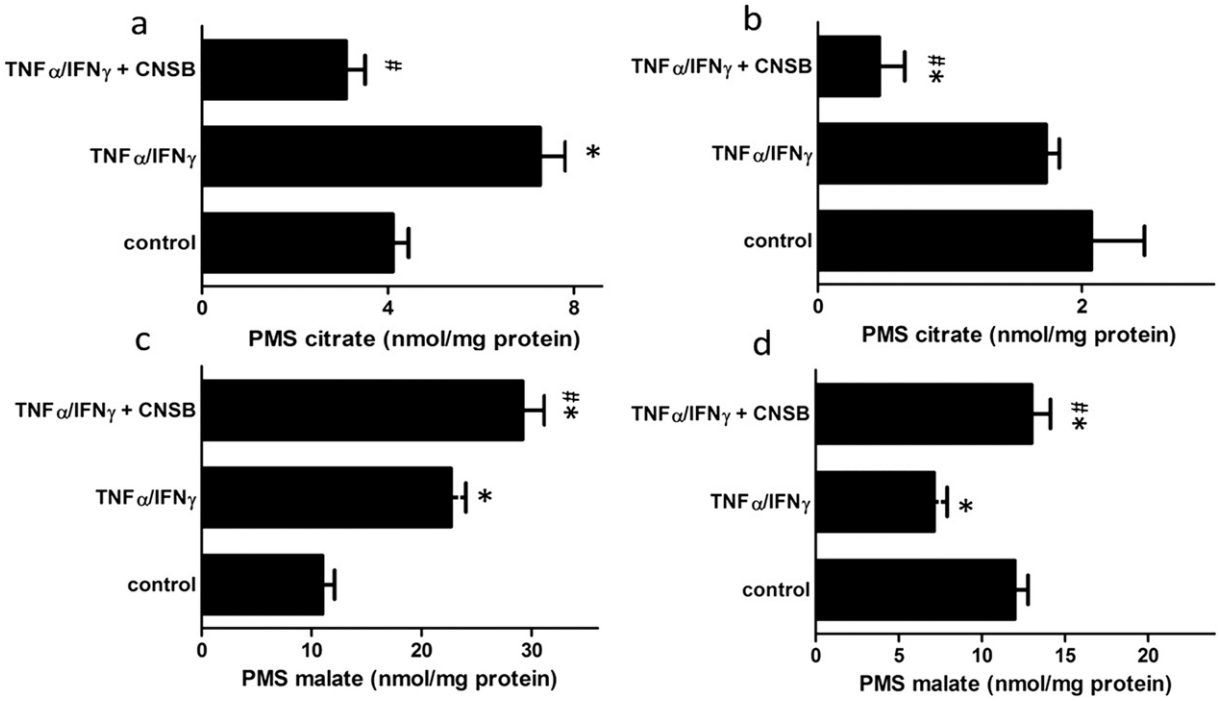

Fig. 7. Citrate and malate levels in PMS of U937 activated cells. U937 cells grown in glucose (a and c) or glucose-free (b and d) medium were activated with TNFα/IFNγ in the presence or absence of CNSB, and PMS were collected. Citrate and malate levels are reported as means ± S.E.M. of at least four independent experiments. The significance of the difference among the citrate or malate levels of activated compared to control cells are indicated (*$p < 0.05$, one-way ANOVA). The significance of the difference among the citrate and malate levels of CNSB-treated compared to those in activated cells not treated with CNSB is indicated. (#$p < 0.05$, one-way ANOVA).

$NADP^+$/NADPH ratio increases in glucose-free but not in glucose-rich medium. This indicates that in absence of glucose activated cells cannot rely on the PPP for NADPH production and become more closely dependent on CIC activity for NADPH production. Activated cells in glucose-free medium contain lower levels of malate in the cytosol compared to those activated in glucose rich medium and CIC inhibition does

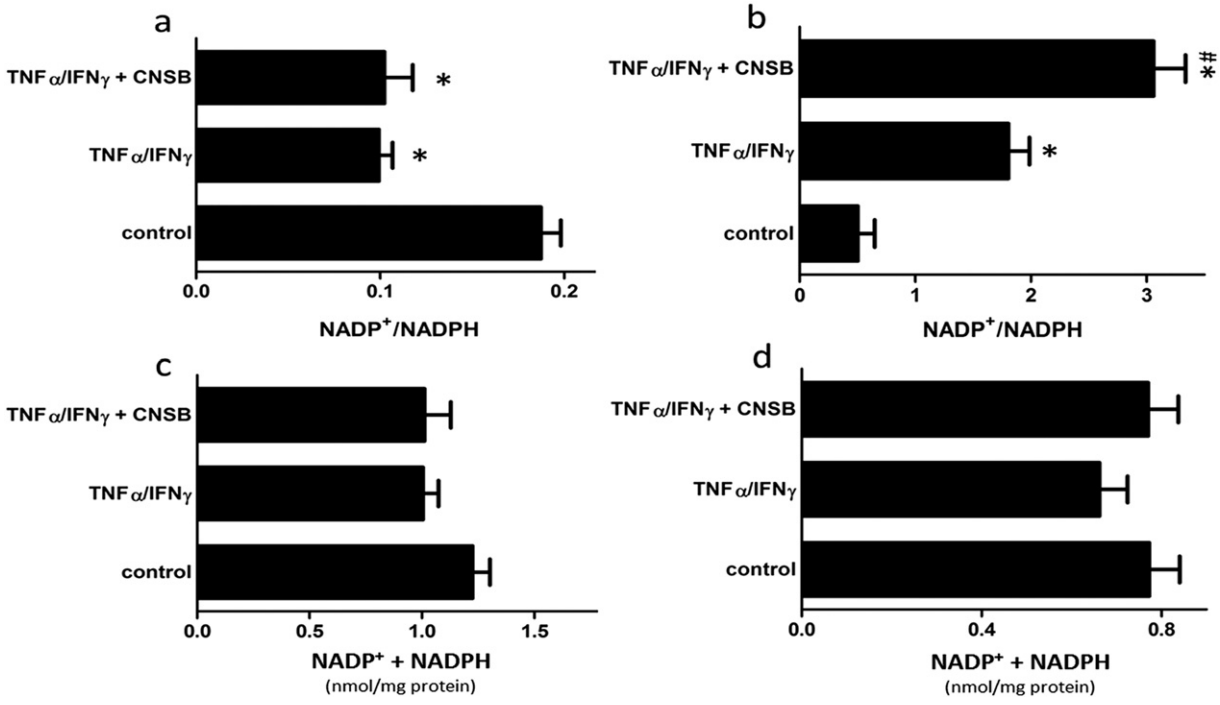

Fig. 8. $NADP^+$/NADPH ratios and ($NADP^+$ + NADPH) total amount in the PMS of U937 activated cells. U937 cells grown in glucose (a and c) or glucose-free (b and d) medium were activated with TNFα/IFNγ in the presence or absence of CNSB and PMS were collected. $NADP^+$/NADPH ratios and the sums of $NADP^+$ + NADPH are reported as means ± S.E.M. of at least four independent experiments. The significance of the difference among the $NADP^+$/NADPH levels of activated compared to control cells are indicated (*$p < 0.05$, one-way ANOVA). The significance of the difference among the $NADP^+$/NADPH levels of CNSB-treated compared to those in activated cells non treated with CNSB is indicated. (#$p < 0.05$, one-way ANOVA).

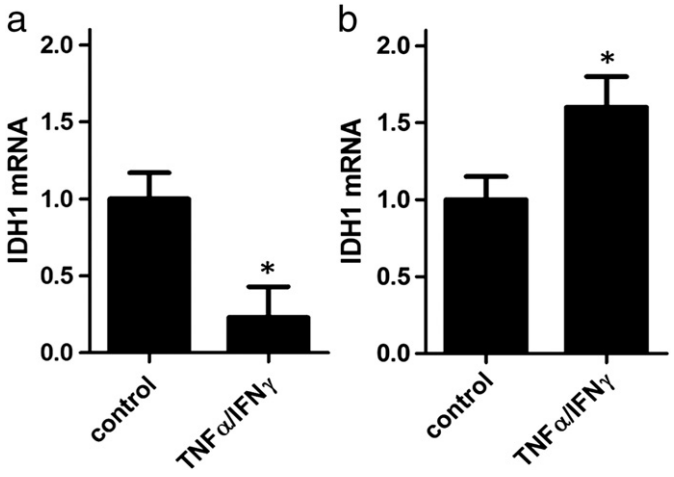

Fig. 9. IDH1 expression in TNFα/IFNγ activated U937 cells. (a) Total RNA from TNFα/IFNγ activated monocytes was used to quantify IDH1 mRNA in the presence (a) or absence (b) of glucose. Means ± S.E.M. of three duplicate independent experiments are shown. Differences between samples and relative controls were significant (*$p < 0.05$, one-way ANOVA).

not produce a strong cytosolic accumulation of malate, indicating that in the absence of glucose cytosolic malate is rapidly consumed by the malic enzyme to produce NADPH. In addition, IDH1 expression levels are increased in U937 cells activated in the absence of glucose, indicating that the citrate conversion to α-oxoglutarate represents an additional route utilized by immune cells to exploit increased citrate efflux for NADPH production. We propose a model in which acetylation/deacetylation equilibrium of CIC represents a cellular mechanism by which the exchange activity of the carrier is rapidly tuned to meet NADPH demand (Fig. 10). In conditions of high glucose levels, activated cells can rely on the PPP to produce NADPH. CIC protein levels are increased, but the levels of acetylated carrier are low (Fig. 10a). During a sustained inflammatory response or with limiting availability of glucose as nutrient, activated cells tune CIC exchange activity by increasing its acetylation (Fig.10b). This modification produces a rapid efflux of citrate in exchange with malate, which is rapidly transported back into the cytosol in exchange with phosphate, probably by the dicarboxylate carrier (DIC) [47], to be rapidly converted to pyruvate by the malic enzyme. In this way the increased citrate/malate exchange driven by acetylation results in a net increase in the efflux of citrate in exchange with phosphate, which re-equilibrates across the inner mitochondrial membrane by recycling on its own transporter [48,49]. The increased net efflux of citrate can simultaneously provide both acetyl-CoA for fatty acid biosynthesis through the ATP-citrate lyase and NADPH necessary to sustain cell functions through IDH1 and malic enzyme (Fig.10b).

K97 is the CIC lysine residue found acetylated in proteomics analyses [1] (http://www.phosphosite.org/proteinAction.do?id=7150&showAllSites=true) putatively directly involved in interactions with citrate. We proposed that its acetylation might improve citrate fitting at the CIC substrate-binding area [4,23]. The replacement of the longer ionic bond with the shorter H-bond does not affect conformational changes and allows a more efficient substrate fitting within the CIC binding site, even favoring a faster uptake and translocation of the CIC substrates without affecting their K_m. It could also be speculated that the acetylation of CIC suggests the presence of mitochondrial acetyl-transferases that can acetylate citrate carrier [50], even if it has also been hypothesized that mitochondrial acetylation could have evolved as a nonenzymatic phenomenon [51-53].

In conclusion, we have provided evidence that the mitochondrial CIC plays an important role in sustaining macrophage function during activation not only for fatty acid (prostaglandins) biosynthesis but also for NADPH production. Acetylation of CIC is a key event increasing the activity of CIC and thereby enhancing the efflux of citrate from mitochondria under specific metabolic conditions. This newly discovered mechanism is likely to be fundamental for macrophage activation, explaining how these cells can maintain the inflammatory mechanisms, when subjected to rapidly changing energy sources in the context of infection or other immune stimuli.

Author contribution and conflict of interest statements

EMR and AC designed the study. EMR, IS, AM and VP performed the experiments. CLP was responsible for the molecular modeling study on CIC. VI provided technical skills and commented on the paper. EMR and

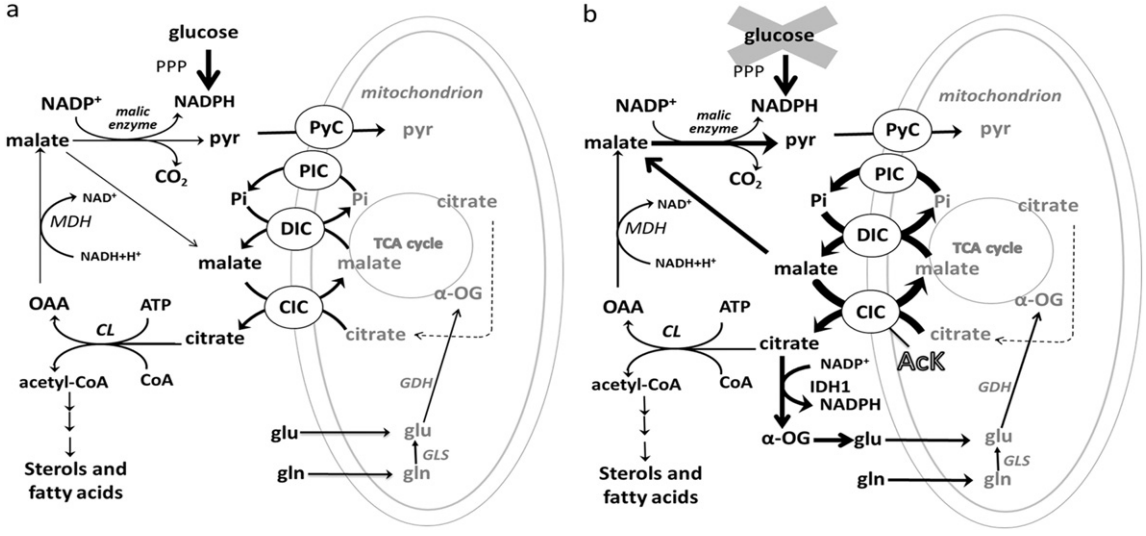

Fig. 10. Role of CIC acetylation in inflammation. During activation of the inflammatory response citrate efflux from mitochondria is necessary to sustain fatty acid biosynthesis. (a) In the presence of glucose, activated immune cells produce NADPH mainly through the pentose phosphate pathway. CIC is maintained in a lower acetylation state, which promotes the efflux of citrate into the cytosol coupled with mitochondrial uptake of malate. (b) In the absence of glucose cells reprogram metabolism to produce NADPH by alternative routes, which are dependent on cytosolic citrate. Increase of CIC acetylation increases efflux of citrate in exchange with malate, which is rapidly transported back to the cytosol by the dicarboxylate carrier (DIC) to be converted to pyruvate. The increased cytosolic amount of citrate can then enter the IDH1 conversion to α-oxoglutarate (α-OG) leading to NADPH production without depauperating fatty acid synthesis. Other abbreviations used: PYC, pyruvate carrier; PIC phosphate carrier; Pi, inorganic phosphate; pyr, pyruvate; glu, glutamate; gln, glutamine; GLS, glutaminase; GDH glutamate dehydrogenase; AcK, acetylated lysine; CL, citrate lyase, IDH1, isocitrate dehydrogenase 1; MDH, malate dehydrogenase; OAA, oxaloacetate.

IS prepared the figures and analyzed the results. DCH provided samples and commented on the paper. VI and FP contributed reagents. AC and FP wrote the paper.

There are no conflicts of interest.

Declaration of interest

The authors declare that there is no conflict of interest that could be perceived as prejudicing the impartiality of the research reported.

Acknowledgments

This work was supported by grants from the Ministerodell'Università dell'Università e della Ricerca (MIUR) and the University of Bari"Aldo Moro" with: This work was supported by the Italian Human ProteomeNet grant no. RBRN07BMCT_009 (MIUR).

References

[1] C. Choudhary, C. Kumar, F. Gnad, M.L. Nielsen, M. Rehman, T.C. Walther, J.V. Olsen, M. Mann, Lysine acetylation targets protein complexes and co-regulates major cellular functions, Science 325 (2009) 834–840.
[2] D.B. Lombard, F.W. Alt, H.L. Cheng, J. Bunkenborg, R.S. Streeper, R. Mostoslavsky, et al., Mammalian Sir2 homolog SIRT3 regulates global mitochondrial lysine acetylation, Mol. Cell. Biol. 27 (2007) 8807–8814.
[3] F. Palmieri, The mitochondrial transporter family SLC25: identification, properties and physiopathology, Mol. Aspects Med. 34 (2013) 465–484.
[4] C.L. Pierri, F. Palmieri, A. De Grassi, Single-nucleotide evolution quantifies the importance of each site along the structure of mitochondrial carriers, Cell. Mol. Life Sci. 71 (2014) 349–364.
[5] F. Bisaccia, A. De Palma, F. Palmieri, Identification and purification of the tricarboxylate carrier from rat liver mitochondria, Biochim. Biophys. Acta 977 (1989) 171–176.
[6] R.S. Kaplan, J.A. Mayor, N. Johnston, D.L. Oliveira, Purification and characterization of the reconstitutively active tricarboxylate transporter from rat liver mitochondria, J. Biol. Chem. 265 (1990) 13379–13385.
[7] F. Bisaccia, A. De Palma, G. Prezioso, F. Palmieri, Kinetic characterization of the reconstituted tricarboxylate carrier from rat liver mitochondria, Biochim. Biophys. Acta 1019 (1990) 250–256.
[8] F. Palmieri, The mitochondrial transporter family (SLC25): physiological and pathological implications, Pflugers Arch. 447 (2004) 689–709.
[9] V. Infantino, P. Convertini, L. Cucci, M.A. Panaro, M.A. Di Noia, R. Calvello, F. Palmieri, V. Iacobazzi, The mitochondrial citrate carrier: a new player in inflammation, Biochem. J. 438 (2011) 433–436.
[10] V. Infantino, V. Iacobazzi, A. Menga, M.L. Avantaggiati, F. Palmieri, A key role of the mitochondrial citrate carrier (SLC25A1) in TNFα- and IFNγ-triggered inflammation, Biochim. Biophys. Acta 1839 (2014) 1217–1225.
[11] P. Newsholme, Why is L-glutamine metabolism important to cells of the immune system in health, postinjury, surgery or infection? J. Nutr. 131 (2001) 2515S–2522S.
[12] F.O. Martinez, S. Gordon, M. Locati, A. Mantovani, Transcriptional profiling of the human monocyte-to-macrophage differentiation and polarization: new molecules and patterns of gene expression, J. Immunol. 177 (2006) 7303–7311.
[13] H. Cimen, M.J. Han, Y. Yang, Q. Tong, H. Koc, E.C. Koc, Regulation of succinate dehydrogenase activity by SIRT3 in mammalian mitochondria, Biochemistry 49 (2010) 304–311.
[14] A. Menga, V. Iacobazzi, V. Infantino, M.L. Avantaggiati, F. Palmieri, The mitochondrial aspartate/glutamate carrier isoform 1 gene expression is regulated by CREB in neuronal cells, Int. J. Biochem. Cell Biol. 60 (2015) 157–166.
[15] M.J. Lindhurst, G. Fiermonte, S. Song, E. Struys, F. De Leonardis, P.L. Schwartzberg, et al., Knockout of Slc25a19 causes mitochondrial thiamine pyrophosphate depletion, embryonic lethality, CNS malformations, and anemia, Proc. Natl. Acad. Sci. U. S. A. 103 (2006) 15927–15932.
[16] F. Palmieri, C. Indiveri, F. Bisaccia, V. Iacobazzi, Mitochondrial metabolite carrier proteins: purification, reconstitution, and transport studies, Methods Enzymol. 260 (1995) 349–369.
[17] F. Bisaccia, C. Indiveri, F. Palmieri, Purification of reconstitutively active alpha-oxoglutarate carrier from pig heart mitochondria, Biochim. Biophys. Acta 810 (1985) 362–369.
[18] I. Stipani, F. Palmieri, Purification of the active mitochondrial tricarboxylate carrier by hydroxylapatite chromatography, FEBS Lett. 161 (1983) 269–274.
[19] G. Fiermonte, V. Dolce, L. David, F.M. Santorelli, C. Dionisi-Vici, F. Palmieri, et al., The mitochondrial ornithine transporter. Bacterial expression, reconstitution, functional characterization, and tissue distribution of two human isoforms, J. Biol. Chem. 278 (2003) 32778–32783.
[20] S. Floyd, C. Favre, F.M. Lasorsa, M. Leahy, G. Trigiante, P. Stroebel, et al., The insulin-like growth factor-I-mTOR signaling pathway induces the mitochondrial pyrimidine nucleotide carrier to promote cell growth, Mol. Biol. Cell 18 (2007) 3545–3555.
[21] F. Palmieri, M. Klingenberg, Direct methods for measuring metabolite transport and distribution in mitochondria, Methods Enzymol. 56 (1979) 279–301.
[22] F. Palmieri, I. Stipani, M. Klingenberg, Kinetic study of the tricarboxylate carrier in rat liver mitochondria, ed: Eur, J. Biochem. 26 (1972) 587–594.
[23] S. Edvardson, A. Ashikov, C. Jalas, L. Sturiale, A. Shaag, A. Fedick, et al., Mutations in SLC35A3 cause autism spectrum disorder, epilepsy and arthrogryposis, J. Med. Genet. 50 (2013) 733–739.
[24] S. Todisco, M.A. Di Noia, A. Castegna, F.M. Lasorsa, E. Paradies, F. Palmieri, The *Saccharomyces cerevisiae* gene YPR011c encodes a mitochondrial transporter of adenosine 5′-phosphosulfate and 3′-phospho-adenosine 5′-phosphosulfate, Biochim. Biophys. Acta 1837 (2014) 326–334.
[25] S. Todisco, G. Agrimi, A. Castegna, F. Palmieri, Identification of the mitochondrial NAD(+) transporter in *Saccharomyces cerevisiae*, J. Biol. Chem. 281 (2006) 1524–1531.
[26] A. Vozza, G. Parisi, F. De Leonardis, F.M. Lasorsa, A. Castegna, D. Amorese, et al., UCP2 transports C4 metabolites out of mitochondria, regulating glucose and glutamine oxidation, Proc. Natl. Acad. Sci. U. S. A. 111 (2014) 960–965.
[27] R. Zallot, G. Agrimi, C. Lerma-Ortiz, H.J. Teresinski, O. Frelin, K.W. Ellens, et al., Identification of mitochondrial coenzyme A transporters from maize and arabidopsis, Plant Physiol. 162 (2013) 581–588.
[28] V. Infantino, A. Castegna, F. Iacobazzi, I. Spera, I. Scala, G. Andria, et al., Impairment of methyl cycle affects mitochondrial methyl availability and glutathione level in Down's syndrome, Mol. Genet. Metab. 102 (2011) 378–382.
[29] A. Castegna, P. Scarcia, G. Agrimi, L. Palmieri, H. Rottensteiner, I. Spera, et al., Identification and functional characterization of a novel mitochondrial carrier for citrate and oxoglutarate in *Saccharomyces cerevisiae*, J. Biol. Chem. 285 (2010) 17359–17370.
[30] V. Iacobazzi, V. Infantino, P. Costanzo, P. Izzo, F. Palmieri, Functional analysis of the promoter of the mitochondrial phosphate carrier human gene: identification of activator and repressor elements and their transcription factors, Biochem. J. 391 (2005) 613–621.
[31] V. Iacobazzi, V. Infantino, F. Palmieri, Epigenetic mechanisms and Sp1 regulate mitochondrial citrate carrier gene expression, Biochem. Biophys. Res. Commun. 376 (2008) 15–20.
[32] L. Palmieri, R. Arrigoni, E. Blanco, F. Carrari, M.I. Zanor, C. Studart-Guimaraes, et al., Molecular identification of an Arabidopsis S-adenosylmethionine transporter. Analysis of organ distribution, bacterial expression, reconstitution into liposomes, and functional characterization, Plant Physiol. 142 (2006) 855–865.
[33] L. Palmieri, A. Vozza, A. Hönlinger, K. Dietmeier, A. Palmisano, V. Zara, et al., The mitochondrial dicarboxylate carrier is essential for the growth of *Saccharomyces cerevisiae* on ethanol or acetate as the sole carbon source, Mol. Microbiol. 31 (1999) 569–577.
[34] L. Palmieri, A. Vozza, G. Agrimi, V. De Marco, M.J. Runswick, F. Palmieri, et al., Identification of the yeast mitochondrial transporter for oxaloacetate and sulfate, J. Biol. Chem. 274 (1999) 22184–22190.
[35] L.F. Costa Rosa, R. Curi, C. Murphy, P. Newsholme, Effect of adrenaline and phorbol myristate acetate or bacterial lipopolysaccharide on stimulation of pathways of macrophage glucose, glutamine and O_2 metabolism. Evidence for cyclic AMP-dependent protein kinase mediated inhibition of glucose-6-phosphate dehydrogenase and activation of NADP+-dependent 'malic' enzyme, Biochem. J. 310 (1995) 709–714.
[36] P. Newsholme, R. Curi, T.C. Pithon Curi, C.J. Murphy, C. Garcia, M. Pires de Melo, Glutamine metabolism by lymphocytes, macrophages, and neutrophils: its importance in health and disease, J. Nutr. Biochem. 10 (1999) 316–324.
[37] A. Haseeb, M.S. Makki, T.M. Haqqi, Modulation of ten-eleven translocation 1 (TET1), Isocitrate Dehydrogenase (IDH) expression, alpha-Ketoglutarate (alpha-KG), and DNA hydroxymethylation levels by interleukin-1beta in primary human chondrocytes, J. Biol. Chem. 289 (2014) 6877-6785.
[38] Y. Xu, J.A. Mayor, D. Gremse, D.O. Wood, R.S. Kaplan, High-yield bacterial expression, purification, and functional reconstitution of the tricarboxylate transport protein from rat liver mitochondria, Biochem. Biophys. Res. Commun. 207 (1995) 783–789.
[39] F. Bisaccia, A. De Palma, T. Dierks, R. Krämer, F. Palmieri, Reaction mechanism of the reconstituted tricarboxylate carrier from rat liver mitochondria, Biochim. Biophys. Acta 1142 (1993) 139–145.
[40] F. Palmieri, C.L. Pierri, Mitochondrial metabolite transport, Essays Biochem. 47 (2010) 37–52.
[41] O.E. Owen, S.C. Kalhan, R.W. Hanson, The key role of anaplerosis and cataplerosis for citric acid cycle function, J. Biol. Chem. 277 (2002) 30409–30412.
[42] E.A. Newsholme, P.H. Sugden, T. Williams, Effect of citrate on the activities of 6-phosphofructokinase from nervous and muscle tissues from different animals and its relationships to the regulation of glycolysis, Biochem. J. 166 (1977) 123–129.
[43] V. Iacobazzi, V. Infantino, F. Bisaccia, A. Castegna, F. Palmieri, Role of FOXA in mitochondrial citrate carrier gene expression and insulin secretion, Biochem. Biophys. Res. Commun. 385 (2009) 220–224.
[44] O. Catalina-Rodriguez, V.K. Kolukula, Y. Tomita, A. Preet, F. Palmieri, A. Wellstein, et al., The mitochondrial citrate transporter, CIC, is essential for mitochondrial homeostasis, Oncotarget 3 (2012) 1220–1235.
[45] V.K. Kolukula, G. Sahu, A. Wellstein, O.C. Rodriguez, A. Preet, V. Iacobazzi, et al., SLC25A1, or CIC, is a novel transcriptional target of mutant p53 and a negative tumor prognostic marker, Oncotarget 5 (2014) 1212–1225.
[46] L.A. O'Neill, D.G. Hardie, Metabolism of inflammation limited by AMPK and pseudo-starvation, Nature 493 (2013) 346–355.
[47] G. Fiermonte, L. Palmieri, V. Dolce, F.M. Lasorsa, F. Palmieri, M.J. Runswick, et al., The sequence, bacterial expression, and functional reconstitution of the rat mitochondrial dicarboxylate transporter cloned via distant homologs in yeast and *Caenorhabditis elegans*, J. Biol. Chem. 273 (1998) 24754–24759.

[48] V. Dolce, V. Iacobazzi, F. Palmieri, J.E. Walker, The sequences of human and bovine genes of the phosphate carrier from mitochondria contain evidence of alternatively spliced forms, J. Biol. Chem. 269 (1994) (Apr 1994) 10451–10460.
[49] G. Fiermonte, V. Dolce, F. Palmieri, Expression in *Escherichia coli*, functional characterization, and tissue distribution of isoforms A and B of the phosphate carrier from bovine mitochondria, J. Biol. Chem. 273 (1998) 22782–22787.
[50] E. Jing, B. Emanuelli, M.D. Hirschey, J. Boucher, K.Y. Lee, D. Lombard, et al., Sirtuin-3 (Sirt3) regulates skeletal muscle metabolism and insulin signaling via altered mitochondrial oxidation and reactive oxygen species production, Proc. Natl. Acad. Sci. U. S. A. 108 (2011) 14608–14613.
[51] B. Osborne, G.J. Cooney, N. Turner, Are sirtuin deacylase enzymes important modulators of mitochondrial energy metabolism? Biochim. Biophys. Acta 1840 (2014) 1295–1302.
[52] S. Ghanta, R.E. Grossmann, C. Brenner, Mitochondrial protein acetylation as a cell-intrinsic, evolutionary driver of fat storage: chemical and metabolic logic of acetyl-lysine modifications, Crit. Rev. Biochem. Mol. Biol. 48 (2013) 561–574.
[53] G.R. Wagner, R.M. Payne, Widespread and enzyme-independent Nε-acetylation and Nε-succinylation of proteins in the chemical conditions of the mitochondrial matrix, J. Biol. Chem. 288 (2013) 29036–29045.